

Activin Type II Receptor Restoration in *ACVR2*-Deficient Colon Cancer Cells Induces Transforming Growth Factor- β Response Pathway Genes

Elena Deacu,¹ Yuriko Mori,¹ Fumiaki Sato,² Jing Yin,¹ Andreea Olaru,¹ Anca Sterian,¹ Yan Xu,¹ Suna Wang,¹ Karsten Schulmann,¹ Agnes Berki,¹ Takatsugu Kan,¹ John M. Abraham,¹ and Stephen J. Meltzer¹

Departments of ¹Medicine, Division of Gastroenterology, and ²Pathology, University of Maryland School of Medicine and Greenebaum Cancer Center and Baltimore VA Hospital, Baltimore, Maryland

Abstract

The *activin type II receptor (ACVR2)* gene is a putative tumor suppressor gene that is frequently mutated in microsatellite-unstable colon cancers (MSI-H colon cancers). *ACVR2* is a member of the transforming growth factor (TGF)- β type II receptor (TGFBR2) family and controls cell growth and differentiation. SMAD proteins are major intracellular effectors shared by *ACVR2* and *TGFBR2* signaling; however, additional shared effector mechanisms remain to be explored. To discover novel mechanisms transmitting the *ACVR2* signal, we restored *ACVR2* function by transfecting wild-type *ACVR2* (wt-*ACVR2*) into a MSI-H colon cancer cell line carrying an *ACVR2* frameshift mutation. The effect of *ACVR2* restoration on cell growth, SMAD phosphorylation, and global molecular phenotype was then evaluated. Decreased cell growth was observed in wt-*ACVR2* transfectants relative to *ACVR2*-deficient vector-transfected controls. Western blotting revealed higher expression of phosphorylated SMAD2 in wt-*ACVR2* transfectants versus controls, suggesting cells deficient in *ACVR2* had impaired SMAD signaling. Microarray-based differential expression analysis revealed substantial *ACVR2*-induced overexpression of genes implicated in the control of cell growth and tumorigenesis, including the activator protein (AP)-1 complex genes *JUND*, *JUN*, and *FOSB*, as well as the small GTPase signal transduction family members, *RHOB*, *ARHE*, and *ARHGDI*. Overexpression of these genes is shared with TGFBR2 activation. This observed similarity between the activin and TGF- β signaling systems suggests that activin may serve as an alternative activator of TGF- β effectors, including SMADs, and that frameshift mutation of *ACVR2* may contribute to MSI-H colon tumorigenesis via disruption of alternate TGF- β effector pathways.

Introduction

The *activin type II receptor (ACVR2)* gene encodes the type II subunit of the activin receptor complex. The type II subunit is essential to activin-mediated signaling; the extracellular binding domain binds to activin, and the intracellular kinase domain activates the type I subunit that activates SMADs (reviewed in ref. 1). Our previous studies detected very frequent frameshift mutations in the A8 tract of exon 10 of *ACVR2* in gastrointestinal cancers with frequent microsatellite instability (MSI-H; colon cancers, 58%; gastric cancers, 44%; ref. 2). Another study identified biallelic mutation of *ACVR2* in 86% of MSI-H colon and pancreatic cancer xenografts and cell lines (3). Loss of *ACVR2* protein was also reported in the majority of MSI-H

tumors harboring frameshift mutation at the polyadenine tract of exon 10 of *ACVR2* (4).

Activin signaling is involved in the regulation of apoptosis, differentiation, proliferation, and cell migration in many tissues, including epithelium, lymphocytes, prostate cancer, breast, vascular endothelium, and liver (reviewed in ref. 1). The activin ligand binds to a heterodimeric transmembrane activin-receptor complex with serine/threonine kinase activity that consists of type I and type II subunits (reviewed in ref. 1). This receptor complex belongs to the transforming growth factor (TGF)- β receptor family and, as does the TGF- β receptor complex, takes the SMAD family of proteins as its downstream signal transducers (5). On binding to activin, the activin-receptor complex phosphorylates SMAD2 and SMAD3 in the cytoplasm, resulting in their activation. Phosphorylated SMADs form a complex with SMAD4 and activate transcription of downstream genes (6).

Some members of the activin signaling pathway have been implicated as tumor suppressor genes. *SMAD4* has been reported as a tumor suppressor in human pancreatic and colon cancers (7). *SMAD2* is mutated in colon and lung cancers (5). Similarly, mutational inactivation of the *activin type I receptor* gene (*ACVR1*) have been observed in pancreatic cancers (8). *SMAD3* null mice develop metastatic colon cancers (9). A dominant negative mutant *ACVR2* also abolishes activin-mediated erythroid differentiation (10). Finally, a recent study showed that activin signaling exerts growth-suppressive effects in colon cancer cells (11).

Microsatellite instability occurring within coding regions underlies tumorigenesis in cancers with frequent microsatellite instability (MSI-H cancers; ref. 12). Frequent frameshift mutations in MSI-H cancers have been reported in *TGFBR2* as well as *ACVR2* (2, 13). To characterize the influence of *ACVR2* gene frameshift mutation on MSI-H colon cancer cells, we analyzed changes in global molecular phenotype after re-expression of constitutively active wild-type (wt)-*ACVR2* using the following: (a) microarray-based gene expression profiling; and (b) analysis of phospho-SMAD2 (p-SMAD2) expression.

Materials and Methods

Plasmid Constructs. The entire coding region of wt-*ACVR2* was PCR-amplified and cloned into the plasmid vector pEF6/V5-His-TOPO (Invitrogen, Carlsbad, CA). The plasmid construct was purified with the HiSpeed Plasmid Midi Kit (Qiagen, Valencia, CA) and analyzed by sequencing and restriction enzyme digestion to confirm the sequence and direction of the insert.

Transfections. The MSI-H colon cancer cell line HCT-15 was used for transfection experiments. HCT-15 carries a biallelic *ACVR2* frameshift mutation at an A8 tract in exon 10 and is inactivated in *TGFBR2* by mutations in both alleles (deletion at an A10 tract in exon 3 and a missense mutation in exon 5; L452P; ref. 14). HCT-15 were cultured in growth medium at 37°C with 5% CO₂. Cells were reseeded in six-well plates at a density of 2.5 × 10⁵ cells per well one day before transfection. Lipofectamine 2000 (Invitrogen) was used to transfect 4 μg of the expression plasmid encoding wt-*ACVR2* as well as control

Received 6/17/04; revised 8/17/04; accepted 9/10/04.

Grant support: CA85069, CA77057, CA95323, CA001808, CA098450, and the Medical Research Office, Department of Veterans Affairs.

The costs of publication of this article were defrayed in part by the payment of page charges. This article must therefore be hereby marked *advertisement* in accordance with 18 U.S.C. Section 1734 solely to indicate this fact.

Note: E. Deacu and Y. Mori contributed equally to this work. Supplementary data for this article can be found at Cancer Research Online at <http://cancerres.aacrjournals.org>.

Requests for reprints: Stephen J. Meltzer, University of Maryland School of Medicine, Division of Gastroenterology, Bressler Research Building, Room 8-009, 655 West Baltimore Street, Baltimore, MD 21201. Phone: (410) 706-3375; Fax: (410) 706-1099; E-mail: smeltzer@medicine.umaryland.edu.

©2004 American Association for Cancer Research.

plasmid containing the *LacZ* gene (pEF6/V5-His-TOPO/*lacZ*). Ten stable wt-*ACVR2* and eight stable vector-control transfectants were selected by expanding single cells in growth media containing 14 $\mu\text{g}/\text{mL}$ Blasticidin S HCl (Invitrogen).

Cell Growth Assay. Direct cell counting was done as follows: Three wt-*ACVR2*-transfected clones and three control vector-transfected clones were plated at a density of 5×10^3 cells per well in 96-well plates in growth media in triplicates at day 0 and counted every day over a 5-day period.

Bromodeoxyuridine (BrdUrd) incorporation assay was done as follows: The experiment was done with Cell Proliferation ELISA BrdUrd (colorimetric) Kit (Roche Applied Science, Indianapolis, IN) according to the manufacturer's protocol. Detailed protocol is available in the Supplementary Methods.

Antibodies. The rabbit polyclonal antibody against *ACVR2* has been produced by Washington Biotechnology (Baltimore, MD). Briefly, two rabbits were twice immunized with a synthetic peptide (NWEKDRNTQGTGVEPCY; 36–51) corresponding to the extracellular domain of *ACVR2*. Six weeks later, the antibodies were affinity chromatography purified from the antisera of the rabbit. Rabbit polyclonal antibodies against *SMAD2/3* and p-*SMAD2* were purchased from Upstate Biotech (Lake Placid, NY) and Cell Signaling Technology (Beverly, MA; used for activin stimulation experiments). Rabbit polyclonal antiactin antibodies were purchased from Santa Cruz Biotechnology Biotech (Santa Cruz, CA).

Western Blotting. Cell lysates were pelleted and then resuspended in 200 μL cell lysis buffer [NaCl 149 mmol/L, NP40 0.01%, Tris 50 mmol/L (pH 7.8), and protease inhibitor cocktail 0.5% (Sigma, St. Louis, MO)]. The protein concentration was determined with the BCA Protein Assay Kit (Pierce, Rockford, IL) with human serum albumin as a standard. The samples were electrophoresed in 10% NuPAGE gel (Invitrogen) and transferred onto polyvinylidene difluoride membrane (Invitrogen). The membranes were immunoblotted with anti-*ACVR2* polyclonal antibody (1:5,000 dilution), anti-*Smad2/3* antibody (2 $\mu\text{g}/\text{mL}$), and antiphosphorylated *Smad2* (1:1,500 dilution). Target protein bands were visualized with ECL Western Blotting detection kit (Amersham Pharmacia Biotech, Piscataway, NJ). The antiactin antibodies were used as a loading control.

For activin stimulation experiments, wt-*ACVR2*- and control vector transfectants were plated in six-well plates at a density of 10^6 cells per well and cultured for 24 hours. The cells were then starved overnight in serum-free medium before the stimulation with 10 or 100 ng of recombinant activin A (Calbiochem, San Diego, CA). The protein extracts from both untreated and treated cells were obtained after 1 or 2 hours of stimulation with PhosphoSafe Extraction Buffer (Novagen, San Diego, CA). HeLa cells treated with 100 ng of TGF- β 1 (Roche Applied Science) were used as a positive control. Thirty 30 micrograms of total protein extracts were electrophoresed and transferred as described above. The membranes were immunoblotted with anti-phospho-*SMAD2* (1 $\mu\text{g}/\text{mL}$) or anti-*SMAD2/3* (1 $\mu\text{g}/\text{mL}$) antibody.

Real-time Quantitative Reverse Transcription (RT)-PCR. Total RNA was extracted with TRIzol reagents (Invitrogen) and was treated with RNase-free DNase on the RNeasy columns (Qiagen).

ACVR2 expression was measured with TaqMan method-based real-time quantitative RT-PCR as described in the Supplementary Methods. β -*actin* was used as a normalization control. The cDNA from untransfected HCT-15 cells was used as a quantification standard. The formula for normalization was as follows: ratio of sample to reference cDNA = $[ACVR2(s)/ACVR2(r)]/[(\beta\text{-actin}(s)/\beta\text{-actin}(r))]$, where *ACVR2*(s) and *ACVR2*(r) were expression levels of *ACVR2* in the samples and reference cDNA, respectively, and β -*actin*(s) and β -*actin*(r) were β -*actin* RNA expression levels in the samples and reference. For validation of microarray results, real-time quantitative one-step RT-PCR analysis was done with Quantitect SYBR Green RT-PCR kit (Qiagen) on iCycler (Bio-Rad, Hercules, CA). Normalization to β -*actin* expression level was done as well.

The sequences of all of the primers and probes are shown in the Supplementary Table 2. Detailed real-time quantitative PCR methods are available in the Supplementary Methods.

Microarray Preparation and Hybridization. Microarray analysis of three wt-*ACVR2*-transfected and three control vector-transfected clones was done as described previously (15). Briefly, amplified RNA was obtained from 20 to 50 μg of total RNA from each clone with a T7-based protocol and was labeled with Cy5 with random primers and reverse transcriptase. The reference sample was a pool of amplified RNAs from eight human malignant cell lines

labeled with Cy3. Each Cy5-labeled specimen probe and the Cy3-labeled reference probe were cohybridized to a microarray slide containing 8,064 sequence-verified human cDNA clones. Probe preparation and hybridization was done individually for each sample clones. After hybridization, each slide was scanned with a GenePix 4000A dual-color slide scanning system (Axon Instruments, Union City, CA).

Data Analysis. We performed both within-slide and between-slide normalization before analysis with LOWESS curve-fitting methods (15). Significance analysis of microarrays was applied to the Lowess-normalized log-scaled data to select genes that were significantly differentially expressed between wt-*ACVR2*-transfected and control vector-transfected clones (15). Significantly differential expression was determined based on significance analysis of microarrays score, a score assigned to each gene on the basis of its fold change of average expression levels between the wt-*ACVR2* transfectants and the control vector transfectants relative to the cumulative SDs of expression levels for wt-*ACVR2* transfectants and control vector transfectants. In this study, only genes with a significance analysis of microarrays score higher than 2 (up-regulation in wt-*ACVR2* transfectants) or smaller than -2 (down-regulation in wt-*ACVR2* transfectants) were classified as significant.

Genes previously related to TGF- β or activin signaling were identified by online database searches. The following web sites were used for this search: PubMed (<http://www.ncbi.nlm.nih.gov>), Stanford SOURCE (<http://genome-www5.stanford.edu/cgi-bin/source/sourceResult>), Human Genome Browser Gateway (<http://genome.ucsc.edu>), and GeneCards (<http://bioinfo.weizmann.ac.il/cards-bin/cardsearch.pl>).

Results

We established a model system for studying wt-*ACVR2* function by reconstituting its activity in HCT-15 colon cancer cells, which are *ACVR2*-deficient secondary to a native biallelic nonsense mutation. We then analyzed the global molecular phenotype of these cells before and after *ACVR2* reconstitution. In addition, we evaluated the impact of *ACVR2* mutation and restoration on its known downstream effector, *SMAD2*.

Confirmation of Successful *ACVR2* Reconstitution. After stable transfection and selection of 18 single-cell clonal transfectants (10 *ACVR2*- and eight control vector-transfected clones), *ACVR2* mRNA levels were measured by real-time quantitative RT-PCR analysis. Measurements in all of the 10 wt-*ACVR2* stable transfectants confirmed that *ACVR2* mRNA levels were higher than in all of the eight control vector-transfected clones, as shown in Fig. 1A. Next, *ACVR2* protein expression level was evaluated by Western blotting. *ACVR2* protein was detectable in all of the 10 wt-*ACVR2* transfectants, and higher levels of *ACVR2* protein were observed in all of the 10 wt-*ACVR2* transfectants than in vector control transfectants (Fig. 1B). On the basis of the data for *ACVR2* mRNA and protein levels, the three wt-*ACVR2* transfectants exhibiting the highest mRNA expression levels were selected for additional analyses.

Effect of *ACVR2* on Cell Growth. Restoration of wt-*ACVR2* function in HCT-15 colon cancer cells resulted in slower cell growth measured by direct cell counting. The difference in growth between wt-*ACVR2* transfectants and control vector transfectants was statistically significant for days 3, 4, and 5 ($P < 0.05$, Student's *t* test; Fig. 2). The calculated doubling time was longer in the wt-*ACVR2*-transfected cells (20 hours) than in the controls (17.4 hours). Additionally, BrdUrd incorporation rate during DNA replication was significantly decreased in wt-*ACVR2* transfectants compared with controls ($P < 0.05$, Student's *t* test; data not shown).

Effect of *ACVR2* on SMAD Signaling. The effect of *ACVR2* mutation and restoration on the known target downstream effector, *SMAD2*, was analyzed by Western blotting. Cell lysates from wt-*ACVR2*-transfected and untransfected (*i.e.*, native mutant) HCT-15 cells were analyzed for expression of both total *SMAD2* and its phosphorylated form (p-*SMAD2*). The p-*SMAD2* expression was higher in wt-*ACVR2*-transfected than in untransfected HCT-15 cells,

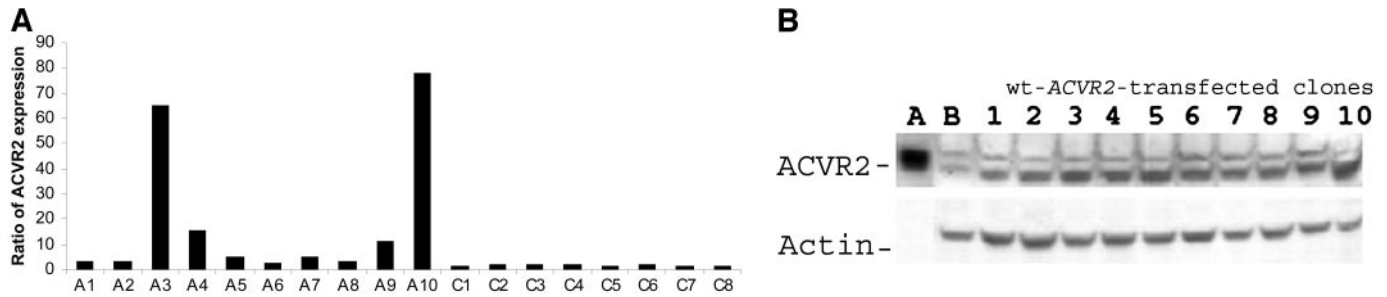


Fig. 1. ACVR2 expression analyses in transfected *versus* untransfected cells. **A**, ACVR2 mRNA levels in transfected cells. A1-A10: wt-ACVR2 transfected cells; C1-C8: positive control vector-transfected cells. Real-time quantitative RT-PCR analysis of ACVR2 mRNA expression levels in 10 wt-ACVR2- and 8 positive control vector-transfected clones revealed significantly higher levels of ACVR2 mRNA in wt-ACVR2 transfected cells (A1-A10) than in controls. Clones A3, A9, and A10 (exhibiting the highest levels of ACVR2 mRNA expression) as well as control clones C1, C2, and C3 were chosen for microarray study. **B**, ACVR2 protein levels in transfected cells. Western blotting analysis of protein lysates was done with a specific anti-ACVR2 antibody. A higher level of ACVR2 expression was seen in all of the 10 wt-ACVR2-transfected clones (Lanes 1–10) than in control vector-transfected cells (Lane B). Recombinant human ACVR2 protein (Sigma-Aldrich, St. Louis, MO) was used as a positive control (Lane A). The blot was then stripped with Restore Western Blot Stripping Buffer (Pierce) and reprobed with antiactin antibodies (Santa Cruz Biotechnology Biotech; bottom row).

whereas total SMAD2 protein levels were identical in both (Fig. 3A). We also evaluated the induction of SMAD2 phosphorylation by activin stimulation. A dose- and time-dependent increase in p-SMAD2 expression was observed in response to activin in wt-ACVR2 transfectants, whereas no effect of activin stimulation on p-SMAD2 level was observed in control vector transfectants (Fig. 3B).

Effect of ACVR2 on Global Molecular Phenotype. To additionally delineate the downstream effects of ACVR2 activation, and to provide insights into candidate downstream pathways discrete from SMAD signaling, we performed gene expression profiling using cDNA microarrays. In these experiments, three clonal wt-ACVR2 transfectants were compared with three clonal control vector transfectants. Significance analysis of microarray was used to select genes that were significantly differentially expressed between these two groups (Table 1; Supplementary Table 1). We eliminated the possibility that modification in gene expression was due to transfection reagents, selection media, or antibiotics by using control vector-transfected clones, rather than parental cells, in this gene expression comparison. ACVR2 expression in wt-ACVR2-transfected cells was the highest of all 8,064 genes on the microarrays. This result was not only expected, but also served as a validation of the cDNA microarray and model system developed in this study.

Genes significantly influenced by wt-ACVR2 transfection are shown in Table 1 (induced genes) and in Supplementary Table 1 (suppressed genes). These included genes induced by growth factors (e.g., *RHOB*, *MAPK6*, *HGS*, and *PPAP2B*); negative regulators of cell proliferation, such as *BTG1*, *PMP22*, or *HGS*; genes implicated in cellular growth regulation (e.g., *CYR61*, *RHOB*, *GPC1*, *JUN*, *INHA*, *PPAP2B*, and *GPC1*); and genes involved in intercellular adhesion (e.g., *CLSTN1*, *LAMP2*, *PVRL3*, *PVRL2*, *MLLT4*, *ARHGDI*). A series of signal transducers, including *ARHE*, *MAPK6*, *LTB*, *PPP2R2C*, *PP1R3A*, *MAP2K3*, *RAB6A*, as well as several regulators of transcription (e.g., *JUN*, *JUND*, *FOSB*, *ATF3*, *JUNB*, *EGRI*, *VGLL1*, *CEBPA*, *MSX1*, and *IRF1*) were also induced by wt-ACVR2. Expression of the transcriptional repressor *ATF3* was increased by wt-ACVR2. Proapoptotic genes such as *NR4A1*, *DUSP2*, and *TNFRSF10C* were overexpressed after wt-ACVR2 restoration, whereas the antiapoptotic gene *BIRC5* was down-regulated.

To validate our microarray results, we performed real-time quantitative RT-PCR analysis. Six genes found to be up-regulated in wt-ACVR2 transfectants by cDNA microarrays (*ARHE*, *ARHGDI*, *CYR61*, *FOSB*, *JUN*, and *JUND*) were analyzed. All six of these genes exhibited increased mRNA levels in wt-ACVR2 transfectants compared with the control vector transfectants, confirming our cDNA microarray results (Supplementary Figure).

Discussion

The involvement of activin signaling disruption in the origin or progression of human digestive tract cancer has been suspected based on the high ACVR2 and ACVR1 mutation rate in various tumors discovered recently (2–4, 8). However, mechanisms of activin signaling and the significance of the ACVR2 mutation in human tumorigenesis have not yet been fully elucidated. Activin and TGF- β share the same receptor binding properties, and their receptors exhibit the same substrate specificity, namely phosphorylation and activation of SMAD2 and SMAD3 (5). Because both TGF- β and activin use the same set of SMADs, it is conceivable that they share common regulatory mechanisms. Therefore, the identification of genes transcriptionally regulated by ACVR2 and elucidation of the molecular mechanisms responsible for this transcriptional regulation will bring us closer to a better understanding of both the activin and TGF- β signaling pathways. Gene expression profiling has been used by a variety of investigators to explore genetic events involving TGF- β signaling (16–19). The current study used this approach to identify new participants in the activin signaling pathway and to explore their commonality with those of the TGF- β signaling pathway.

Initially, we evaluated the effect of restoration of wt-ACVR2 function in a colon cancer cell line, HCT-15, carrying a biallelic ACVR2 frameshift mutation at the mutational hotspot where the majority of human primary MSI-H digestive tract cancers demonstrate ACVR2

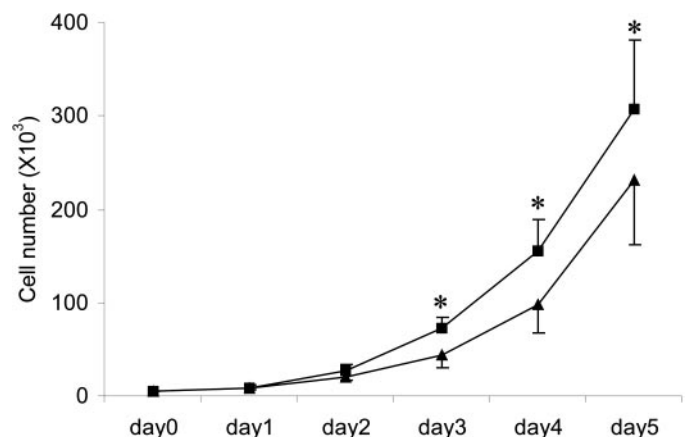


Fig. 2. Cell growth assay of the wt-ACVR2 transfectants and control vector transfectants. This line graph displays results of direct cell counting over a 5-day period. The plots represent triplicate measurements for three wt-ACVR2 transfectants (▲) and three control vector transfectants (■); bars, \pm SD. The wt-ACVR2 transfectants showed significantly slower growth compared with control transfectants (*, measurement with $P < 0.05$, Student's t test).

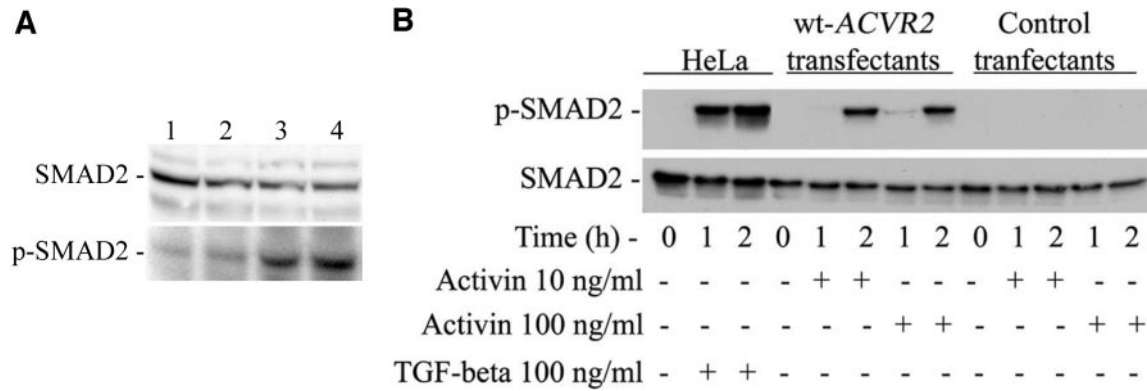


Fig. 3. SMAD2 protein expression and phosphorylation analyses in HCT15 colon cancer cells. *A*, SMAD2 and p-SMAD2 protein expression in wt-ACVR2 vector-transfected and untransfected cells. Immunoblotting was done with anti-SMAD2/3 and anti-p-SMAD2 antibodies. Total SMAD2 protein levels were equal in untransfected (*top row, Lanes 1 and 2*) and wt-ACVR2-transfected (*top row, Lanes 3 and 4*) HCT-15 cells. However, levels of p-SMAD2 protein were higher in wt-ACVR2-transfected cells (*bottom row, Lanes 3 and 4*) than in untransfected cells (*bottom row, Lanes 1 and 2*). This finding suggests that ACVR2 frameshift mutation results in impaired phosphorylation of SMAD2 proteins. *B*, activin-induced SMAD2 phosphorylation in wt-ACVR2 transfectants and control vector transfectants. Protein extracts were obtained from untreated (*time 0*) and from activin-treated cells after 1 and 2 hours of stimulation (*time 1 and 2*). Increased levels of p-SMAD2 were detected in wt-ACVR2 transfectants with the highest level after 2 hours of activin treatment, whereas no p-SMAD2 was detected in the control vector transfectants. HeLa cells untreated and treated with 100 ng of TGF- β 1 were used as a positive control. Immunoblotting to anti-SMAD2 antibodies was done on the same membrane as anti-p-SMAD2 antibody immunoblotting after stripping of the previous antibody. Total SMAD2 protein levels were identical in both untreated and activin treated wt-ACVR2 transfectants as well as in control vector transfectants. The positions of signals detected by anti-p-SMAD2 and anti-SMAD2 antibodies were identical, additionally verifying the identity of the protein detected by anti-p-SMAD2 antibody.

frameshift mutation (2–4). We showed that restoration of activin signaling by wt-ACVR2 transfection in this cell line resulted in increased SMAD2 phosphorylation in response to activin stimulation. This finding establishes that this biallelic mutation impairs signal transduction and implicates loss of ACVR2-mediated SMAD signaling in MSI-H colon cancer. Furthermore, the restoration of wt-ACVR2 function caused decreased cell growth in MSI-H colon cancer cells *in vitro*.

Global molecular phenotyping revealed numerous similarities between signaling via TGFBR2 and via ACVR2. For example, the AP-1 complex members including FOS and JUN have been implicated in signaling initiated by TGF- β (20). In the current study, AP-1 complex members JUN, JUND, JUNB, and FOSB were up-regulated by wt-ACVR2, suggesting that activin and TGF- β signaling share AP-1 involvement as effector mechanisms. Phosphorylated JUN and JUND have higher DNA-binding affinities than their nonphosphorylated counterparts, making them logical targets for the phosphorylation-mediated signaling shared by TGFBR2 and ACVR2 (20). Moreover, JUND is an inhibitor of normal intestinal mucosal growth *in vivo* and plays a critical role in the negative control of epithelial cell renewal under physiologic and pathological conditions (21). Similarly, JUN is a regulator of transcription, cell growth and maintenance, and interacts with the SMAD3/4 heterodimer (20). Another newly observed similarity between ACVR2 and TGFBR2 signaling concerns the up-regulation of genes induced or activated by growth factors. For example, the Rho protein family member RHOB is rapidly induced by TGF- β , epidermal growth factor, and platelet-derived growth factor (22). In the current study, RHOB was up-regulated in wt-ACVR2 transfectants. RHOB is an immediate-early gene implicated in growth control as a potent inhibitor of malignant transformation as well as a suppressor of tumor growth and has been suggested to be a novel mechanism of tumor suppression by TGF- β (18, 19, 22). Interestingly, two other genes involved in Rho protein signaling, ARHE and ARHGDI, were also up-regulated in wt-ACVR2 transfectants. Transcriptional repressor ATF3 is a TGF- β -inducible factor that forms a complex with SMAD3 (23). ATF3 expression was found to be increased by TGF- β but not by bone morphogenetic protein (23). In the current study, ATF3 was overexpressed in wt-ACVR2 transfectants, suggesting that activin is another TGF- β family member that

can induce the expression of ATF3. Finally, in the current study, wt-ACVR2 restoration up-regulated a growth factor-inducible immediate-early protein, CYR61, that promotes proliferation, migration, and adhesion, which was known to be similarly up-regulated by TGFBR1 and ACVR1 (19).

Furthermore, the current study revealed a number of genes that have not previously been implicated in TGFBR2 signaling. For example, up-regulation by wt-ACVR2 was observed for the proapoptotic genes NR4A1, DUSP2, and TNFRSF10C in addition to down-regulation of the antiapoptotic gene BIRC5. Increased expression of negative regulators of cell proliferation, including BTG1, PMP22, and TOB2 after wt-ACVR2 restoration was observed as well. Additionally, the following genes were also up-regulated by wt-ACVR2 transfection: MAPK6, a gene activated in response to growth factors through protein phosphorylation; HGS, a negative regulator of cell proliferation that undergoes tyrosine phosphorylation in response to epidermal growth factor and platelet-derived growth factor; and PPAP2B, a growth control gene that is known to be enhanced by epidermal growth factor in HeLa cells (24–26).

Recently, significant progress has been made toward identifying signal transduction pathways activated by TGF- β receptor family members. However, fewer studies have been published regarding the downstream effectors of activin receptors. In the present study, we focused our attention on ACVR2-regulated genes. We combined examination of the SMAD-mediated signaling pathway with gene expression profiling. Among genes identified as influenced by ACVR2 restoration, some had previously been related to TGF- β receptor signaling, whereas others were not previously suspected in either the ACVR2 or TGFBR2 pathways. The observed strong similarity between the activin and TGF- β signaling systems suggests that activin serves as an alternative activator of downstream TGF- β effectors in addition to SMADs. In addition, we confirmed that restoration of wt-ACVR2 function resulted in decreased cell growth and increased SMAD2 phosphorylation in a MSI-H colon cancer cell line with native biallelic ACVR2 frameshift mutation. Taken together, these data suggest that activin may serve as an alternative activator of SMADs and other downstream TGF- β effectors and that frameshift mutation of ACVR2 may contribute to MSI-H colon tumorigenesis via disruption of alternate TGF- β effector pathways.

Table 1 *Genes upregulated in wt-ACVR2 transfectants classified according to their involvement in biological processes*

Gene symbol	Description	Accession no.	SAM score	Fold change
ACVR2	Activin type II receptor	NM001616	8.47	160.93
Apoptosis				
PEA15	Phosphoprotein enriched in astrocytes 15	NM003768	3.51	2.42
TNFRSF10C	Decoy receptor 1 (DcR1)	NM003841	2.94	3.08
DUSP2	Dual specificity phosphatase 2/PAC1	NM004418	4.06	9.96
NR4A1	NAK1 DNA binding protein	NM002135	4.68	2.52
CyCS	Cytochrome c	NM018947	2.76	2.14
SGK	Serine/threonine protein kinase sgk	NM005627	2.52	1.72
Regulation of transcription				
JARID1C	SMC (mouse) homolog, X chromosome (SMCX)	NM004187	4.47	1.69
JUN	V-jun avian sarcoma virus 17 oncogene homolog (JUN)	NM002228	3.76	5.26
JUND	Jun D proto-oncogene	NM005354	6.42	2.82
FOSB	FBJ murine osteosarcoma viral oncogene homolog B	NM006732	3.26	5.82
KIAA0551	TRAF2 and NCK interacting kinase	AB011123	3.97	1.64
TBX2	T-box 2	NM005994	3.37	1.85
ATF3	Activating transcription factor 3	NM001674	2.64	2.95
EGR1	Early growth response 1 (EGR1)	NM001964	2.44	2.41
VGLL1	TONDU (TONDU)/vestigial like 1 (Drosophila)	NM016267	2.40	2.31
JUNB	Jun B proto-oncogene	NM002229	2.40	1.79
CEBPA	CCAAT/enhancer binding protein (C/EBP), α	NM004364	2.39	2.42
MSX1	Msh (Drosophila) homeo box homolog 1	NM002448	2.62	1.88
HCA58	Hepatocellular carcinoma-associated antigen 58	AF220416	2.43	2.15
RELA	V-rel avian reticuloendotheliosis viral oncogene homolog A	L19067	2.36	1.70
IRF1	Interferon regulatory factor 1	NM002198	2.23	1.61
TLE3	Transducin-like enhancer protein 3/KIAA1547 protein	NM005078	3.15	1.96
Cell growth and/or maintenance				
RHOB	Ras homolog gene family, member B	NM004040	3.86	3.91
CYR61	Cysteine-rich, angiogenic inducer, 61	NM001554	6.21	6.5
GPC1	Glypican 1	NM002081	6.21	2.10
EXTL1	Tumor suppressor EXT-like protein	NM001440	3.59	2.00
NFKB2	Nuclear factor of κ light polypeptide gene enhancer in B-cells 2 (p49/p100)	NM002502	3.04	2.04
PPAP2B	Phosphatidic acid phosphatase 2b	NM003713	3.99	2.02
JUN	V-jun avian sarcoma virus 17 oncogene homolog	NM002228	3.76	5.26
INH1A	Inhibin A	NM002191	3.32	1.81
SLC3A2	Solute carrier family 3 (activators of dibasic and neutral amino acid transport), member 2	NM002394	2.29	2.32
Signal transduction				
ARHE	Ras homolog gene family, member E (RhoE)	NM005168	3.27	2.54
MAPK6	Mitogen-activated protein kinase 6/ERK3	NM002748	3.46	1.70
LTB	Lymphotoxin β	NM002341	3.55	3.09
EDN1	Endothelin 1	NM001955	3.51	2.53
PPP2R2C	Protein phosphatase 2, regulatory subunit B γ isoform	XM029744	2.76	1.61
CAPN5	Calpain5	NM004055	2.54	1.81
MAP2K3	MAP kinase kinase 3b	NM145110	2.38	2.10
PLCB4	Phospholipase C, β 4	NM000933	2.62	1.91
RAB6A	RAB6A, member RAS oncogene family	NM002869	2.58	1.52
NR2F1	Nuclear receptor subfamily 2, group F, member 1	NM005654	2.48	1.75
TBL3	Transducin β -like 3	NM006453	2.29	1.87
PPP1R3A	Protein phosphatase 1, regulatory (inhibitor) subunit 3A	XM054777	2.24	1.68
Cell adhesion				
ARHGDI1A	Rho GDP dissociation inhibitor α (RhoDHIA)	NM004309	4.12	3.20
CLSTN1	KIAA0911 protein	NM014944	3.72	2.00
LAMP2	Lysosomal-associated membrane protein 2	NM002294	2.98	2.44
PVRL3	Nectin 3	NM015480	2.72	2.41
PVRL2	Poliovirus receptor-related 2 (herpes virus entry mediator B)	NM002856	2.66	2.39
ATP2A2	ATPase, Ca ⁺⁺ transporting, cardiac muscle, slow twitch 2	NM001681	2.36	1.58
MLLT4	Myeloid/lymphoid or mixed-lineage leukemia (trithorax homolog, Drosophila); translocated to, 4	NM005936	2.33	1.97
VEL1	Vertebrate LIN7 homolog 1, Tax interaction protein 33	NM004664	2.88	2.54
Regulation of cell proliferation				
BTG1	B-cell translocation gene 1, antiproliferative	NM001731	3.58	2.02
PMP22	Peripheral myelin protein 22	NM000304	3.52	2.01
HGS	Hepatocyte growth factor-regulated tyrosine kinase substrate	NM004712	3.06	1.84
LRPAP1	Low density lipoprotein-related protein-associated protein 1	NM002337	3.60	1.96
IGF2	Insulin-like growth factor 2 (somatomedin A)	NM000612	3.09	3.22
DYRK1A	Serine-threonine protein kinase (MNBH)	NM101395	2.49	1.91
TOB2	Transducer of ERBB2, 2	NM016272	2.37	1.84
Cell-cell signaling				
GIP2	Interferon-stimulated protein, 15 kDa (ISG15)	NM005101	2.78	2.90

Table 1 *Continued*

Gene symbol	Description	Accession no.	SAM score	Fold change
RNA processing				
CHERP	Protein with polyglutamine repeat; calcium (ca2+) homeostasis endoplasmic reticulum protein	NM006387	5.98	2.92
MPHOSPH10	M-phase phosphoprotein 10	NM005791	3.09	1.76
SLBP	Hairpin binding protein, histone (HBP)	NM006527	2.50	2.25
Intercellular junction assembly				
GJA7	Gap junction protein, α 7, 45kD (connexin 45)	NM005497	2.54	2.39
Transport				
ATP7B	ATPase, Cu ⁺⁺ transporting, β polypeptide (Wilson disease)	NM000053	4.10	6.14
ATP6IP1	ATPase, H ⁺ transporting, lysosomal, subunit 1	NM001183	3.76	1.80
SLC16A1	Monocarboxylate transporter 1 (SLC16A1)	NM003051	3.07	1.65
ATP6V0C	ATPase, H ⁺ transporting, lysosomal (vacuolar proton pump)	NM001694	3.04	1.50
GTF3C1	General transcription factor III C, polypeptide 1 (α subunit)	NM001520	3.90	1.83
TLOC1	Translocation protein 1	NM003262	3.13	2.17
NAPG	N-ethylmaleimide-sensitive factor attachment protein, γ	NM003826	2.29	2.32
Metabolism				
ALDH1A1	Aldehyde dehydrogenase 1 family, member A1	NM000689	3.89	5.20
AUP1	Ancient ubiquitous protein 1	AF100754	3.71	1.72
ATP1A1	ATPase, Na ⁺ /K ⁺ transporting, α 1 polypeptide	NM000701	3.28	1.50
AGPAT2	Lysophosphatidic acid acyltransferase	NM006412	2.52	3.07
RNA binding				
RBM12	Putative brain nuclearly-targeted protein	AB018308	3.77	1.96
EIF2S1	Translation initiation factor eIF-2α	NM004094	2.93	1.67
FMR1	Fragile X mental retardation 1	NM002024	2.32	2.06
Protein modification				
PLOD3	Procollagen-lysine 2-oxoglutarate 5-dioxygenase	NM001084	3.66	2.35
PTPRU	Receptor protein tyrosine phosphatase hPTP-J precursor	NM005704	3.37	1.73
Proteolysis and peptidolysis				
WFDC2	WAP four-disulfide core domain 2	NM006103	2.54	2.49
C1S	Complement component 1, s subcomponent	NM001734	2.50	3.30
PSMD13	Proteasome (prosome, macropain) 26S subunit	NM002817	2.62	1.66
PRSS8	Prostasin	NM002773	2.40	1.73
Cytoskeletal anchoring				
VIL2	Vilin2	NM003379	3.11	2.07
SDC3	Syndecan 3 (N-syndecan)	AB007937	2.26	2.04
PLEC1	Plectin 1	NM000445	2.25	1.75
Regulation of cell migration				
SERPINE2	Plasminogen activator inhibitor type 1 member	NM006216	2.60	3.67
Heat shock protein activity				
SERPINH2	Collagen binding protein 2	NM001235	2.98	2.08
HSPH1	Heat shock M_r 105,000 (HSP105B)	NM006644	2.85	3.65
DNAJB1	Heat shock M_r 40,000 protein 1 (HSPF1)	NM006145	3.10	2.19
HSPA6	Heat shock M_r 70,000 protein 6 (HSP70B')	NM002155	2.49	2.29
Defense response				
TFF3	Trefoil factor 3 (intestinal)	NM003226	2.51	2.51
Nucleosome assembly				
HIST1H1C	H1 histone family, member 2 (H1F2)	NM005319	2.47	3.62
Others				
HMOX1	Heme oxygenase (decycling) 1	NM002133	2.41	2.42
CDR2	Cerebellar degeneration-related protein 2	BC017503	2.97	2.20
A2LP	Ataxin 2 related protein	NM007245	2.94	2.04
PCOLN3	Procollagen (type III) N-endopeptidase	NM002768	2.83	1.55
RNF13	Ring finger protein 13	NM007282	2.43	1.96
IER2	Immediate early protein (ETR101)	NM004907	2.91	2.80
HCA58	Hepatocellular carcinoma-associated antigen 58	AF220416	2.43	2.15

NOTE. Fold change is the average of the relative expression ratios for the three wt-ACVR2-transfectants to the reference probe divided by the average of the relative expression ratios for the three vector control transfectants to the reference probe. Bold represents genes previously reported by various studies as related to TGF- β signaling pathway (16–19, 23).

References

1. Chen YG, Lui HM, Lin SL, Lee JM, Ying SY. Regulation of cell proliferation, apoptosis, and carcinogenesis by activin. *Exp Biol Med (Maywood)* 2002;227:75–87.
2. Mori Y, Sato F, Selaru FM, et al. Instability typing reveals unique mutational spectra in microsatellite-unstable gastric cancers. *Cancer Res* 2002;62:3641–5.
3. Hempen PM, Zhang L, Bansal RK, et al. Evidence of selection for clones having genetic inactivation of the activin A type II receptor (ACVR2) gene in gastrointestinal cancers. *Cancer Res* 2003;63:994–9.
4. Jung B, Doctolero RT, Tajima A, et al. Loss of activin receptor type 2 protein expression in microsatellite unstable colon cancers. *Gastroenterology* 2004;126:654–9.
5. Eppert K, Scherer SW, Ozcelik H, et al. MADR2 maps to 18q21 and encodes a TGFbeta-regulated MAD-related protein that is functionally mutated in colorectal carcinoma. *Cell* 1996;86:543–52.
6. Lagna G, Hata A, Hemmati-Brivanlou A, Massague J. Partnership between DPC4 and SMAD proteins in TGF-beta signalling pathways. *Nature (Lond)* 1996;383:832–6.
7. Hahn SA, Schutte M, Hoque AT, et al. DPC4, a candidate tumor suppressor gene at human chromosome 18q21.1. *Science (Wash DC)* 1996;271:350–3.
8. Su GH, Bansal R, Murphy KM, et al. ACVR1B (ALK4, activin receptor type 1B) gene mutations in pancreatic carcinoma. *Proc Natl Acad Sci USA* 2001;98:3254–7.
9. Zhu Y, Richardson JA, Parada LF, Graff JM. Smad3 mutant mice develop metastatic colorectal cancer. *Cell* 1998;94:703–14.
10. Liu F, Shao LE, Yu J. Truncated activin type II receptor inhibits erythroid differentiation in K562 cells. *J Cell Biochem* 2000;78:24–33.
11. Jung B, Beck S, Fiorino A, et al. Functional correlation of growth suppression with activin treatment in microsatellite unstable, activin type 2 receptor (ACVR2)-restored colorectal cancer cells. *Gastroenterology* 2004;126:A264.
12. Perucho M. Cancer of the microsatellite mutator phenotype. *Biol Chem* 1996;377:675–84.
13. Markowitz S, Wang J, Myeroff L, et al. Inactivation of the type II TGF-beta receptor in colon cancer cells with microsatellite instability. *Science (Wash DC)* 1995;268:1336–8.
14. Ilyas M, Efstathiou JA, Straub J, Kim HC, Bodmer WF. Transforming growth factor beta stimulation of colorectal cancer cell lines: type II receptor bypass and changes in adhesion molecule expression. *Proc Natl Acad Sci USA* 1999;96:3087–91.
15. Mori Y, Selaru FM, Sato F, et al. The impact of microsatellite instability on the molecular phenotype of colorectal tumors. *Cancer Res* 2003;63:4577–82.
16. Verrecchia F, Chu ML, Mauviel A. Identification of novel TGF-beta /Smad gene targets in dermal fibroblasts using a combined cDNA microarray/promoter transactivation approach. *J Biol Chem* 2001;276:17058–62.
17. Zavadil J, Bitzer M, Liang D, et al. Genetic programs of epithelial cell plasticity directed by transforming growth factor-beta. *Proc Natl Acad Sci USA* 2001;98:6686–91.
18. Xie L, Law BK, Aakre ME, et al. Transforming growth factor beta-regulated gene expression in a mouse mammary gland epithelial cell line. *Breast Cancer Res* 2003;5:R187–98.
19. Ryu B, Kern SE. The essential similarity of TGFbeta and activin receptor transcriptional responses in cancer cells. *Cancer Biol Ther* 2003;2:164–70.
20. Zhang Y, Feng XH, Derynck R. Smad3 and Smad4 cooperate with c-Jun/c-Fos to mediate TGF-beta-induced transcription. *Nature (Lond)* 1998;394:909–13.
21. Li L, Liu L, Rao JN, et al. JunD stabilization results in inhibition of normal intestinal epithelial cell growth through P21 after polyamine depletion. *Gastroenterology* 2002;123:764–79.
22. Du W, Prendergast GC. Geranylgeranylated RhoB mediates suppression of human tumor cell growth by farnesyltransferase inhibitors. *Cancer Res* 1999;59:5492–6.
23. Kang Y, Chen CR, Massague J. A self-enabling TGFbeta response coupled to stress signaling: Smad engages stress response factor ATF3 for Id1 repression in epithelial cells. *Mol Cell* 2003;11:915–26.
24. Boulton TG, Nye SH, Robbins DJ, et al. ERKs: a family of protein-serine/threonine kinases that are activated and tyrosine phosphorylated in response to insulin and NGF. *Cell* 1991;65:663–75.
25. Komada M, Kitamura N. Growth factor-induced tyrosine phosphorylation of Hrs, a novel 115-kilodalton protein with a structurally conserved putative zinc finger domain. *Mol Cell Biol* 1995;15:6213–21.
26. Perou CM, Jeffrey SS, van de Rijn M, et al. Distinctive gene expression patterns in human mammary epithelial cells and breast cancers. *Proc Natl Acad Sci USA* 1999;96:9212–7.